

Exact Volumes of Semi-Algebraic Convex Bodies

Lakshmi Ramesh*

Universität Bielefeld

Bielefeld, Germany

lramesh@math.uni-bielefeld.de

Nicolas Weiss†

Max Planck Institute for Mathematics in the Sciences

Leipzig, Germany

nicolas.weiss@mis.mpg.de

Abstract

We compute the volumes of convex bodies that are given by inequalities of concave polynomials. These volumes are found to arbitrary precision thanks to the representation of periods by linear differential equations. Our approach rests on work of Lairez, Mezzarobba, and Safey El Din. We present a novel method to identify the relevant critical values. Convexity allows us to reduce the required number of creative telescoping steps by an exponential factor. We provide an implementation based on the `ore_algebra` package in SageMath. This is applied to a problem in geometric statistics, where the convex body is an intersection of ℓ_p -balls.

Keywords

Semi-algebraic sets; Picard-Fuchs equations; Symbolic-numeric algorithms; Volume computation; Holonomic functions

1 Introduction

In this paper, we compute exact volumes of semi-algebraic convex bodies defined by finitely many concave polynomials. This is motivated by geometric statistics, where intersections of convex bodies arise as maximum likelihood estimator (MLE) sets. The statistical model proposed by Koltchinskii, Ramesh and Wahl in [10] considers a convex body $K + \theta$, that is K translated by θ , and random variables X_1, \dots, X_k uniformly distributed on $K + \theta$. The MLE set is then the bounded convex set

$$C = \bigcap_{i=1}^k (K + X_i). \quad (1)$$

One can think of the MLE set as a higher-dimensional analog of the confidence interval. In fact, it estimates the unknown parameter θ with 100% confidence level. That is, θ is necessarily in C . This certainty is complemented by a large MLE set. What one means by *large* must be made precise.

The *size* of the MLE set can be measured in many ways, such as the diameter in the case of [10]. In most cases, one can only provide estimates or bounds. However, if K is a semi-algebraic set, the volume of the MLE set can be computed accurately up to any chosen number of decimal digits.

The examples considered in [10] are ℓ_p -balls and their intersections in \mathbb{R}^n . These objects are not only basic semi-algebraic sets, but the polynomials that define them are also concave functions. In this article, we will focus on semi-algebraic convex bodies of the form

$$C = \{x \in \mathbb{R}^n \mid f_1(x) > 0, \dots, f_k(x) > 0\} \quad (2)$$

*The research of L.R. is funded by the Deutsche Forschungsgemeinschaft (DFG, German Research Foundation) – project number 539663130

†The research of N.W. is funded by the European Union (ERC, UNIVERSE PLUS, 101118787). Views and opinions expressed are, however, those of the author(s) only and do not necessarily reflect those of the European Union or the European Research Council Executive Agency. Neither the European Union nor the granting authority can be held responsible for them.

where $f_i \in \mathbb{Q}[x_1, \dots, x_n]$ are concave. Then, the common positivity locus of the polynomials f_i is the intersection of each of their convex supports, and hence also convex. We will in short refer to this class as *semi-algebraic convex bodies*.

Classically, the volume of semi-algebraic sets is approximated using probabilistic methods, such as the Monte Carlo method. If one samples points uniformly from a box containing the set C , then the ratio

$$\frac{\#\{\text{samples in } C\}}{\#\{\text{all samples}\}} \xrightarrow{\text{converges to}} \frac{\text{vol}(C)}{\text{vol}(\text{Box})}$$

as the number of samples goes to infinity. The rate of convergence however is $N^{-1/2}$, due to the central limit theorem, which is slow for high-precision computations. To obtain a precision of 4 decimal digits with high probability then requires 10^8 samples.

The Monte Carlo method is based on a very physical understanding of the volume of a set and is a probabilistic method. Instead, we use a deterministic approach rooted in an algebraic understanding of volumes as integrals.

Consider for example the ℓ_4 -ball C in \mathbb{R}^3 . Its volume can be given in closed form using the Γ -function:

$$\begin{aligned} \text{vol}(C) &= \frac{(2\Gamma(1 + 1/4))^3}{\Gamma(1 + 3/4)} \\ &= 6.481987351786382022151846056460487... \end{aligned}$$

This number is a *period*, which means it is the value of a definite integral. We are interested in computing periods that do not have a closed form such as the one above.

The exact computation of volumes of compact semi-algebraic sets with arbitrary precision was addressed by Lairez, Mezzarobba, and Safey El Din in [12]. They realize the volumes of semi-algebraic sets as periods of rational integrals [11]. Moreover, the volume can then be computed up to arbitrary precision by numerically solving a corresponding univariate linear differential equation, called a Picard-Fuchs equation. Illustrations of this technique can be found in [18, § 2] and it fits into the broader framework of metric algebraic geometry [3, Ch. 14].

We apply this to compute volumes of semi-algebraic convex bodies, and in this setting provide improvements to the algorithm in [12]. We reduce the required steps by a factor that is exponential in the dimension by focusing only on a single interval given by two critical values of a projection. We do this by introducing a new method to select the relevant critical values.

We provide the first full implementation [15] of the algorithm. It is written primarily in SageMath [20] and uses the `ore_algebra` package by Kauers, Jaroschek and Johansson [9]. We also incorporate additional software, namely `msolve` [1], `Macaulay2` [7], and the Julia [2] package `HypersurfaceRegions.jl` based on [16].

Our article has the following outline. In Section 2, we review the necessary results from the theory of holonomic functions that allow

us to view the volume of C as the analytic continuation of volumes of deformed sets, each of whose volumes can be computed as a definite integral. The computation is done by solving corresponding differential equations. We elaborate on the algorithm applied to our class of semi-algebraic convex bodies. In Section 3, we focus on the convexity of this class, which is closed under deformations and slices of deformations. This property guarantees the existence of only two relevant critical values for any projection in the recursive algorithm. We discuss our methods to compute these relevant critical values. Finally, in Section 4, we elaborate on the improvement with respect to complexity of our implementation. We discuss examples of volumes and the Picard–Fuchs operators that arise in our computations. We also discuss questions that arise from these examples and opportunities for improvements of the algorithm.

Acknowledgments

We are grateful to Eric Pichon-Pharabod for his help in understanding the software systems involved. We thank Leonie Kayser and Mohab Safey El Din for useful discussions. We are also grateful to Anna-Laura Sattelberger for her continuous support. And finally we thank Bernd Sturmfels for encouraging us to pursue this project.

2 Volumes via differential equations

Notation. We denote by $D_{t,x}$ (and $R_{t,x}$) the Weyl algebra (and rational Weyl algebra) of linear differential operators with coefficients in $\mathbb{Q}[t, x_1, \dots, x_n]$ (and $\mathbb{Q}(t, x_1, \dots, x_n)$). We denote the action of a linear differential operator $P \in D_{t,x}$ on a differentiable function φ by $P \bullet \varphi$. The absence of a bullet indicates multiplication. The notation $\text{Ann}_{D_{t,x}}(\varphi)$ refers to the left-ideal in $D_{t,x}$ of linear differential operators P such that $P \bullet \varphi = 0$. If $\frac{p}{q}$ is the leading coefficient of P , then $\deg(P) := \deg(p) - \deg(q)$. We may denote (x_1, \dots, x_n) with \mathbf{x} .

The fundamental starting point for computing volumes using differential operators is a shift in perspective. While, of course, the volume $\text{vol}(C)$ can be realized as an integral in \mathbb{R}^n of the constant function 1 over C itself, it is much more useful to describe it as an integral over a closed integration contour in \mathbb{C}^n as follows.

LEMMA 2.1. *Let $C = \{x \in \mathbb{R}^n \mid f(x) > 0\}$ be a bounded region of \mathbb{R}^n given by a single polynomial $f \in \mathbb{Q}[x_1, \dots, x_n]$ and assume that its vanishing set $V(f)$ is a smooth variety. Then, the volume of the semi-algebraic set C is a period of the rational function*

$$A(x) = \frac{(\partial_{x_1} \bullet f)x_1}{f}. \quad (3)$$

That is,

$$\text{vol}(C) = \frac{1}{2\pi i} \int_{\Gamma} A(x) dx_1 \wedge \dots \wedge dx_n \quad (4)$$

where Γ is a closed cycle $\Gamma \subset \mathbb{C}^n - \partial C$.

The proof is based on Stokes' theorem and Leray's residue theorem [14, III, Thm. 2.4], a higher-dimensional generalization of Cauchy's integral theorem, which explains the factor of $1/(2\pi i)$. The explicit shape of Γ , which is the Leray coboundary ∂C , is not actually required to know. Only that the contour is closed becomes

relevant below. Also, the choice of x_1 is arbitrary since for a different x_i , the integrand is a cohomologous differential form on the complement of $V(f)$.

This distinct viewpoint becomes powerful, when the periods depend on an additional parameter t , so that they not only describe individual values, such as $\text{vol}(C)$, but functions $\varphi(t)$ such that $\text{vol}(C) = \varphi(t_{\text{val}})$ for some value $t_{\text{val}} \in \mathbb{Q}$.

Definition 2.2. For an open set $U \subset \mathbb{C}$, a function $\varphi : U \rightarrow \mathbb{C}$ is said to be a *period of a rational function dependent on t* if there exists a rational function $A \in \mathbb{C}(t, x_1, \dots, x_n)$ such that for every $p \in U$, there exists a neighborhood of p where $\varphi(t)$ can be written as

$$\varphi(t) = \int_{\Gamma} A(t, x) dx_1 \wedge \dots \wedge dx_n \quad (5)$$

for a closed cycle Γ that is independent of t and lies in the complement of the poles of $A(t, x)$.

We will see below in Proposition 2.5 that volumes of semi-algebraic sets can be represented by periods of rational functions depending on a single parameter. Theorem 2.4 then implies that the exact volume can be obtained by numerically solving a linear differential equation

$$p_n(t) \frac{d^n \varphi}{dt^n}(t) + \dots + p_1(t) \frac{d\varphi}{dt}(t) + p_0(t) \varphi(t) = 0$$

with $p_0, \dots, p_n \in \mathbb{C}[t]$ for a specific solution $\varphi(t)$ up to arbitrary precision. Note that this linear differential equation can be equivalently written as

$$P \bullet \varphi(t) = 0 \quad \text{where} \quad P = \sum p_i \partial_t^i \in D_t.$$

To explain the existence of a non-zero linear differential operator P that annihilates the periods of a rational function, we recall for the reader's convenience the necessary parts from the theory of holonomic functions and D -ideals.

A function in a single variable x_1 is *holonomic* if there exists a non-zero linear differential operator $P \in D_{x_1}$ that annihilates it. A function f in n variables is *holonomic* if there exists a holonomic left ideal I [17, Def. 1.4.8] in the Weyl algebra $D_{\mathbf{x}}$ such that all operators $P \in I$ annihilate f . We refer to such an ideal as an *annihilating ideal* for f . In practice, to show that a function f is holonomic, it suffices to provide an ideal $I \subset \text{Ann}_{R_{\mathbf{x}}}(f) \subset R_{\mathbf{x}}$ of finite holonomic rank since its Weyl closure $D_{\mathbf{x}} \cap I$ will be a holonomic annihilating ideal in $D_{\mathbf{x}}$ [17, Thm. 1.4.15]. For more background on holonomic functions, we refer the reader to [18].

Example 2.3 (Rational functions are holonomic). A rational function $A \in \mathbb{Q}(x_1, \dots, x_n)$ is holonomic since it is annihilated by the operator $A\partial_i - \partial_i \bullet A$ for all i and the ideal

$$I = \langle A\partial_i - \partial_i \bullet A \rangle \subset R_{\mathbf{x}} \quad (6)$$

has holonomic rank 1. Hence, its Weyl closure

$$J := D_{\mathbf{x}} \cap I \quad (7)$$

is a holonomic $D_{\mathbf{x}}$ -ideal annihilating A .

Fundamental operations on functions, such as restrictions and integration, have analogous operations at the level of their annihilating D -ideals. For integration, the main theoretical statement is the following. It is presented in similar form in [17, Thm. 5.5.1].

THEOREM 2.4. *Let $J \subset D_{t,x}$ be an annihilating ideal of a rational function $A \in \mathbb{Q}(t, \mathbf{x})$. Then, the ideal*

$$\mathcal{I}_t(J) := (J + \partial_{x_1} D_{t,x} + \cdots + \partial_{x_n} D_{t,x}) \cap D_t \quad (8)$$

annihilates periods of A that depend on the parameter t .

If J is holonomic, then also its integration ideal $\mathcal{I}_t(J)$ is holonomic by [19, Thm. 6.10.3]. It follows then that periods of rational functions depending on a parameter are holonomic. In our case, recall (5), $A(t, \mathbf{x})$ is a holonomic function, and therefore J as in Example 2.3 is holonomic. Hence, also the integration ideal $\mathcal{I}_t(J)$ is holonomic. This implies that there is a non-zero univariate linear differential operator $P \in D_t$ and operators $Q_i \in D_{t,x}$, such that

$$P - \partial_{x_1} Q_{x_1} - \cdots - \partial_{x_n} Q_{x_n} \in \text{Ann}_{D_{t,x}}(A). \quad (9)$$

It follows from this presentation that P annihilates the definite integral in (5).

PROOF OF THEOREM 2.4. Suppose P and the Q_1, \dots, Q_n are given as above. Then,

$$0 = \int_{\Gamma} (P - \partial_{x_1} Q_{x_1} - \cdots - \partial_{x_n} Q_{x_n}) \bullet A(t, \mathbf{x}) dx_1 \wedge \cdots \wedge dx_n.$$

Since P does not depend on the integration variables it can be taken out of the integral. Furthermore, each of the remaining terms vanish by Stokes' theorem. It is applicable, since $Q_{x_i} \bullet A$ defines a smooth function on the complement of the poles of A since $Q_{x_i} \in D_{t,x}$. \square

The process of computing operators of the form (9) is called *creative telescoping* [21]. P is called the *telescopers* and the operators Q_i are called the *certificates*. In practice, creative telescoping is often done iteratively by integrating out a single variable at a time. That is, given J , at each step, one computes

$$\mathcal{I}_{t,x_1, \dots, x_i}(J) = (\mathcal{I}_{t,x_1, \dots, x_{i+1}}(J) + \partial_{x_{i+1}} D_{t,x_1, \dots, x_{i+1}}) \cap D_{t,x_1, \dots, x_i}. \quad (10)$$

In each iterative step, telescopers and their respective certificates are computed. We refer the reader to [8, Sec. 5.4] and [6] for details on the various creative telescoping algorithms available.

The final operator P in (9) is called a *Picard–Fuchs operator*, a non-zero linear differential operator in D_t which annihilates periods of $A \in \mathbb{Q}(t, \mathbf{x})$ depending on t .

Now consider concave polynomials $f_1, \dots, f_k \in \mathbb{Q}[x_1, \dots, x_n]$. They define the convex, compact semi-algebraic set

$$C = \bigcap_{i=1}^k \{x \in \mathbb{R}^n \mid f_i(x) > 0\}. \quad (11)$$

Moreover, C can be described as the limit (in the Hausdorff metric) of the 1-parameter family of semi-algebraic sets

$$C_t = \{x \in \mathbb{R}^n \mid \prod_i f_i(x) - t > 0\} \cap C. \quad (12)$$

Since the deformed product

$$F_t := f_1 \cdot \dots \cdot f_k - t \in \mathbb{Q}[t, \mathbf{x}] \quad (13)$$

has nowhere vanishing Jacobian, it follows that its vanishing set $V(F_t) \subset \mathbb{R}^{n+1}$ is a smooth variety. By Sard's theorem, also the slice $V(F_t) \cap \{t\} \times \mathbb{R}^n$ is smooth for all but finitely many values of t . This then also holds for a connected component of $V(F_t)$, such as the boundary of C_t , which we denote by ∂C_t . We will refer to C_t as the (smooth) *deformation* of C .

PROPOSITION 2.5 ([12, THM. 2]). *Let C_t be defined as in (12). Then*

$$\varphi : (0, \varepsilon) \rightarrow \mathbb{R}, \quad t \mapsto \text{vol}(C_t) \quad (14)$$

is a period of a rational integral depending on the parameter t for small $\varepsilon > 0$. Moreover, $\text{vol}(C)$ is the analytic continuation of $\varphi(t)$ to $t = 0$.

This shows that the volume function $\varphi(t)$ is a solution of a Picard–Fuchs operator P_t in D_t . In the above, ε can be chosen to be the smallest positive singular value of t for P_t . Locally, on simply connected regions away from the singular locus of P_t , the solutions of P_t form a \mathbb{C} -vector space of dimension $\text{ord}(P_t)$. Thus, our particular solution $\varphi(t)$ can be specified in this vector space by providing suitable initial conditions. By [12, Lemma 15], the initial conditions can be of the following form:

LEMMA 2.6. *The solution of P_t , which realizes $\varphi(t) = \text{vol}(C_t)$ on an open interval $(0, \varepsilon)$, can be uniquely determined by providing the value of $\text{vol}(C_t)$ at $\text{ord}(P_t)$ many suitable points $t \in (0, \varepsilon)$.*

Once φ is determined within the solution space of P_t on $(0, \varepsilon)$, the volume of C is then obtained by analytically continuing φ to $t = 0$. The word "suitable" in Lemma 2.6 has to be understood as follows. Along a path $\gamma : t_0 \rightarrow t_1$ outside the singular locus of a linear differential operator P , analytic continuation provides an isomorphism of the \mathbb{C} -vector space of solutions Sol_{t_0} at t_0 , and Sol_{t_1} at t_1 . This isomorphism can be described in a suitable basis and can be computed numerically, for example using high-precision solvers such as implemented in the `ore_algebra` package up to arbitrary precision. Providing the value $\text{vol}(C_t)$ at a point t_i only fixes a single coordinate in Sol_{t_i} . The $\text{ord}(P_t)$ many values for t are then suitable, if together they determine, namely as a linear system, all coordinates in Sol_{t_0} uniquely.

Let us now describe how the values of $\text{vol}(C_t)$ can be determined recursively as volumes of lower-dimensional semi-algebraic sets. By a *slice* of C_t , we mean the intersection of C_t with a hyperplane. Since the boundary of a slice of smooth set is also smooth, one can make a more general statement about slices of C_t and their volumes.

PROPOSITION 2.7 ([12, THM. 7]). *If $f \in \mathbb{Q}[x_1, \dots, x_n]$ such that the boundary of $C = \{x \in \mathbb{R}^n \mid f(x) > 0\}$ is smooth, then for C a union of bounded, connected components of C , the volume of the slice*

$$\varphi(v) = \text{vol}(C \cap \{x \in \mathbb{R}^n \mid x_i = v\})$$

is a period of the rational function

$$A = \frac{(\partial_{x_j} \bullet f(x_i = v))x_j}{f(x_i = v)}, \quad \text{for any } i \neq j, \quad (15)$$

on any open interval of adjacent critical values of the projection

$$\text{pr}_{x_i} : \partial C \rightarrow \mathbb{R}, \quad \mathbf{x} \mapsto x_i. \quad (16)$$

Let $(c_1, c_2) \subset \mathbb{R}$ be such an interval of adjacent critical values for C_t . The volume of C_t over this interval can be computed by evaluating the integral

$$\psi(s) = \int_{c_1}^s \text{vol}(C_t \cap \{x \in \mathbb{R}^n \mid x_i = v\}) dv \quad (17)$$

at $s = c_2$. By Proposition 2.7, the integrand is annihilated by a Picard–Fuchs operator $P \in D_{x_i}$. Therefore, by the fundamental theorem of calculus, it follows that

$$P\partial_{x_i} \bullet \psi = 0. \quad (18)$$

As before for φ , one can solve for ψ by providing suitable initial conditions, this time in terms of the values of $\psi'(s)$, which is the volume of the slice over $x_i = s$.

This leads to an algorithm that computes the volume integral (5) as a solution of a Picard–Fuchs operator. Since solving the Picard–Fuchs operator requires initial conditions which are volume computations of lower-dimensional slices, the algorithm is recursive with depth n . Algorithm 1 takes as input k concave polynomials and returns the volume of C to a chosen precision. It implicitly calls Algorithm 2, a recursive algorithm that computes the volume of the deformed convex body. Algorithms 1 and 2 were presented in more general form in [12]. The two algorithms make use of several subroutines, which will only be shortly described in this section:

- **CreativeTelescoping(I, x_i)**: Returns an element P of the integration ideal of I that integrates out all variables but x_i , using a suitable creative telescoping algorithm. See also Section 4.
- **SuitableValues($P, (a, b)$)**: Returns a list for suitable values for $x_i \in (a, b)$ to uniquely determine a solution of P on (a, b) . See also Section 3.
- **Solve($P, L_{ic}, x_i = v$)**: Determines the solution φ of P by the list of initial conditions L_{ic} and returns its value $\varphi(x_i = v)$ for a value $v \in [a, b]$.

Algorithm 1 VolumeSemiAlgebraic

Input: Concave polynomials $f_1, \dots, f_k \in \mathbb{Q}[x_1, \dots, x_n]$, precision $N \in \mathbb{N}$.
Output: Volume of the convex body C up to N binary digits.

```

 $F_t := \prod_i f_i - t$ 
 $A_t := \frac{(\partial_1 \bullet F_t) x_1}{F_t}$ 
 $I_t := \langle A \partial_\alpha - \partial_\alpha \bullet A \mid \alpha \in \{x_1, \dots, x_n, t\} \rangle$ 
 $P_t := \text{CreativeTelescoping}(I_t, t)$ 
 $L_t := \text{SuitableValues}(P_t, (0, \varepsilon))$ 
 $L_{ic} := \text{empty list of InitialConditions}$ 
for  $t_{\text{val}} \in L_t$  do
  append( $L_{ic}$ , SmoothVolume( $(f_1, \dots, f_k), t_{\text{val}}, N$ ))
end for
 $\text{vol}_0 := \text{Solve}(P_t, L_{ic}, t = 0)$ 
return  $\text{vol}_0$ 

```

- **CriticalValues** : $((f_1, \dots, f_k), t_{\text{val}}, x_{\text{pr}})$: Returns the critical values of the projection from $\partial C_{t_{\text{val}}}$ onto the x_{pr} axis. We will prove in Section 3, that for the class of concave polynomials there will only be two such critical values. How to obtain them is described in Algorithm 3.
- **1DimVolume** ($L_{\text{res}}, t_{\text{val}}, N$): Returns the 1-dim volume of the deformed intersection, assuming that the restricted polynomials in L_{res} are univariate, see also Section 3.

- **ProjectionVariable** ($(f_1, \dots, f_k), t_{\text{val}}$): Selects one of the available variables to project onto next. This becomes relevant in Section 4.

Algorithm 2 SmoothVolume

Input: Concave polynomials (f_1, \dots, f_k) in $\mathbb{Q}[x_1, \dots, x_n]$, deformation value $t_{\text{val}} \in \mathbb{Q}$, number of precision bits $N \in \mathbb{N}$.
Output: Volume of the deformation $C_{t_{\text{val}}}$ up to N binary digits.

```

 $x_{\text{pr}} := \text{ProjectionVariable}((f_1, \dots, f_k), t_{\text{val}})$ 
 $F_{t_{\text{val}}} := \prod_i f_i - t_{\text{val}}, \quad A := \frac{(\partial_{x_i} \bullet F_{t_{\text{val}}}) x_i}{F_{t_{\text{val}}}}$  for  $x_i \neq x_{\text{pr}}$ 
 $I := \langle A \partial_i - \partial_i \bullet A \mid 1 \leq i \leq n \rangle$ 
 $P := \text{CreativeTelescoping}(I, x_{\text{pr}})$ 
 $c_1, c_2 := \text{CriticalValues}((f_1, \dots, f_k), t_{\text{val}}, x_{\text{pr}})$ 
 $L := \text{SuitableValues}(P, (c_1, c_2))$ 
 $L_{ic} := \text{empty list of InitialConditions}$ 
for  $x_{\text{val}} \in L$  do
   $L_{\text{res}} := (f_1, \dots, f_k)(x_{\text{pr}} = x_{\text{val}})$ 
  if  $n > 2$  then
    append( $L_{ic}, \varphi'(x_{\text{val}}) = \text{SmoothVolume}(L_{\text{res}}, t_{\text{val}}, N)$ )
  else ( $n = 2$ )
    append( $L_{ic}, \varphi'(x_{\text{val}}) = \text{1DimVolume}(L_{\text{res}}, t_{\text{val}}, N)$ )
  end if
end for
return  $\text{Solve}(P \partial_{x_{\text{pr}}}, L_{ic}, x_{\text{pr}} = c_2)$ 

```

3 Convex Sets and Their Deformations

A polynomial $f \in \mathbb{Q}[x]$ is a concave function on a convex set $U \subseteq \mathbb{R}^n$ if for any $x, y \in U$ and $\alpha \in [0, 1]$

$$f(\alpha x + (1 - \alpha)y) \geq \alpha f(x) + (1 - \alpha)f(y). \quad (19)$$

LEMMA 3.1. Let $U \subset \mathbb{R}^n$ be a convex region and $f : U \rightarrow \mathbb{R}$ a concave function on that region. Then for any t , the super-levelset

$$f_{>t} := \{x \in \mathbb{R}^n \mid f(x) > t\} \quad (20)$$

is a convex subset of \mathbb{R}^n .

PROOF. This is an immediate consequence of the definition of concavity. If for $x, y \in U$, both $f(x) > t$ and $f(y) > t$, then this holds by definition for any point along the line segment connecting x and y . \square

Let now $f_1, \dots, f_k \in \mathbb{Q}[x]$ be a list of concave polynomials. Then their common positivity locus

$$C = \bigcap_{i=1}^k \{x \in \mathbb{R}^n \mid f_i(x) > 0\} \quad (21)$$

is a convex subset of \mathbb{R}^n .

Example 3.2. Fix an even integer $p \in 2\mathbb{N}_{>0}$. Consider the unit ℓ_p -ball in \mathbb{R}^n , centered at μ . It is a semi-algebraic set given by the concave polynomial

$$f_{\ell_p, \mu} = 1 - ((x_1 - \mu_1)^p + \dots + (x_n - \mu_n)^p). \quad (22)$$

We denote the corresponding translated ℓ_p -ball by $C_{\ell_p, \mu} := (f_{\ell_p, \mu})_{>0}$. Given μ_1 and μ_2 , if $C := C_{\ell_p, \mu_1} \cap C_{\ell_p, \mu_2} \neq \emptyset$, then C is one out of two connected components of $(f_{\ell_p, \mu_1} f_{\ell_p, \mu_2})_{>0}$. Figure 1 shows the

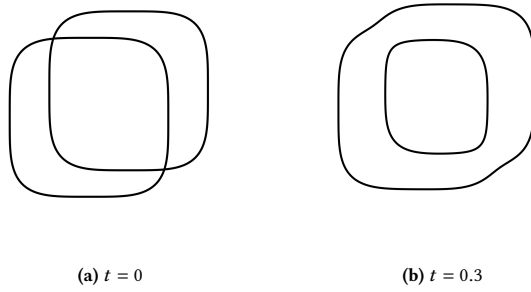
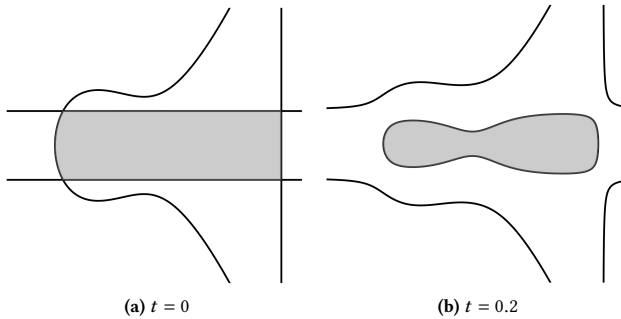
Figure 1: Two ℓ_4 -balls deformed by a parameter t 

Figure 2: Convex set with non-convex deformation

deformation of two ℓ_4 -balls in \mathbb{R}^2 centered at $(0, 0)$ and $(1/2, 1/3)$. The deformed product is given then by

$$F_t = (1 - x^4 - y^4)(1 - (x - 1/2)^4 - (y - 1/3)^4) - t, \quad (23)$$

and $C_t \subseteq (F_t)_{>0}$. Figure 1(a) shows $V(F_t(t = 0))$ and 1(b) shows $V(F_t(t = 0.3))$.

Let us now study the deformed intersection C_t . For general polynomials, even though for small t the deformation C_t is connected, its slices may have multiple components, as the following example shows.

Example 3.3. Consider the semi-algebraic set $C \subset \mathbb{R}^2$ defined by the common positivity locus of

$$f := -(y^2 - (x + 1)x^2 - \frac{1}{2})$$

and the three affine linear polynomials

$$l_1 := -(x - 2), \quad l_2 := (y + \frac{1}{2}), \quad l_3 := -(y - \frac{1}{2}).$$

In this case, the semi-algebraic set C , depicted in gray in Figure 2(a), is convex. However, its deformation C_t , seen in gray in Figure 2(b) for $t = 0.2$ is not. In particular, there exists some value v at which the slice at $y = v$ has two connected components.

For concave polynomials, we can guarantee that the deformation C_t , and hence all its slices, are convex for all t .

PROPOSITION 3.4. *Let C be the common positivity locus of concave polynomials $f_1, \dots, f_k \in \mathbb{Q}[\mathbf{x}]$. Then, its deformation C_t as defined in (12) is a convex set for all $t > 0$.*

PROOF. Since each of the polynomials f_i was assumed to be concave on \mathbb{R}^n , it follows that they are also concave on the common positivity locus which is given by C .

The deformations C_t are the super-levelsets of the product $F := \prod_{i=1}^k f_i$ that are contained in C . Hence, it suffices to show that F is a concave function when restricted to the convex set C . Since the logarithm is a strictly monotonic function, we can equivalently show that

$$\log(F) = \log(f_1) + \dots + \log(f_k)$$

is a concave function on C . But this follows since by the defining Equation (19), sums of concave functions are concave. \square

It naturally follows from this observation that for any x_i , the projection of the boundary of the deformed intersection ∂C_t onto the x_i -axis has exactly two critical values, namely the minimum and maximum of x_i attained on C_t . Moreover, Proposition 3.4 and this conclusion hold true for any non-empty slice obtained by transverse intersection with an affine hyperplane since concave functions are naturally preserved under restriction to affine-linear subspaces.

Consider now the projection onto the x_i -axis. The map

$$\text{pr}_{x_i} : \partial C_t \rightarrow \mathbb{R}, \quad \mathbf{x} \rightarrow x_i \quad (24)$$

has precisely two critical values $c_1 < c_2 \in \mathbb{R}$ and the function

$$\varphi : \mathbb{R} \rightarrow \mathbb{R}, \quad v \rightarrow \text{vol}(C_{t,x_i=v}) \quad (25)$$

is a period of a rational function when φ is restricted to the open interval $(c_1, c_2) \subset \mathbb{R}$.

Let us now describe how the implementation of the routines `CriticalValues` and `1DimVolume` profits from the setting of of concave polynomials.

CriticalValues. The critical values coming from ∂C_t can be identified among the critical values coming from the projection of the vanishing set of F_t in the following way. We suppose that $t \in \mathbb{Q}_{>0}$ is fixed, so that $F_t \in \mathbb{Q}[\mathbf{x}]$. Then, the locus of critical points `CritPts` of the projection of the algebraic set $V(F_t) \subset \mathbb{R}^n$ is the vanishing set of the ideal

$$I = \langle \tilde{F}_t, \partial_{x_1} \bullet \tilde{F}_t, \dots, \widehat{\partial_{x_i} \bullet \tilde{F}_t}, \dots, \partial_{x_n} \bullet \tilde{F}_t \rangle \quad (26)$$

where \tilde{F}_t denotes the square-free part of F_t and where the i^{th} derivative is omitted. The critical values `CritValsi` of the projection of F_t on to the x_i -axis are then obtained by elimination. The two relevant critical values corresponding to the projection of ∂C_t can be identified in two possible ways:

Case 1 ($\dim(\text{CritPts}) = 0$): In this case, there are only finitely many points in the locus of critical points. We check which of them lie in C by evaluating each of the f_i 's. By the convexity of C_t shown in Proposition 3.4 and since $\dim(\text{CritPts}) = 0$, we know that there will be exactly two such critical points. By projecting them back onto the x_i -axis, we have found the two relevant critical values.

Case 2 ($\dim(\text{CritPts}) > 0$): In this case, we consider the hypersurface arrangement

$$V(F_t) = \bigcup_{s \in \text{CritVals}_i} \{x \in \mathbb{R}^n \mid x_i = s\}. \quad (27)$$

We begin by sampling one point from each region of the complement of the hypersurface arrangement. We identify the sampled points that lie in the deformed intersection C_t , and project them onto the x_i -axis. This set of projected values defines a closed interval $[a, b]$. Then, the points in CritVals_i that are closest to but outside to either side of $[a, b]$ are the critical values of the projection of C_t onto the x_i -axis.

Algorithm 3 CriticalValues

Input: Concave polynomials $f_1, \dots, f_k \in \mathbb{Q}[\mathbf{x}]$, projection variable x_i , deformation value $t_{\text{val}} \in \mathbb{Q}_{>0}$.
Output: Critical values c_1, c_2 of the projection $\text{pr}_{x_i} : \partial C_{t_{\text{val}}} \rightarrow \mathbb{R}$.
 $f := \text{SquareFree}(\prod f_i - t_{\text{val}})$
 $I := \langle f, \partial_1 \bullet f, \dots, \partial_n \bullet f \rangle$
 $\langle p_{\text{cv}} \rangle = \text{Eliminate}(I, x_1, \dots, \widehat{x}_i, \dots, x_n)$
if $\dim(I) = 0$ **then**
 $\text{CritPts} := \text{msolve}(I)$
 $a, b = \text{Pts} \cap C$
 $c_1, c_2 = \text{pr}_{x_i}(a, b)$
else
 $\text{CritVals} := \text{Roots}(p_{\text{cv}}, \mathbb{R})$
 $\text{pts} := \text{SamplePoints}(\text{HypersurfaceRegions}(p_{\text{cv}} \cdot f))$
 $c_1 := \max\{p \in \text{CritVals} \mid p < \min(\text{pr}_{x_i}(\text{pts} \cap C_{t_{\text{val}}}))\}$
 $c_2 := \min\{p \in \text{CritVals} \mid p > \max(\text{pr}_{x_i}(\text{pts} \cap C_{t_{\text{val}}}))\}$
end if
return $\{c_1, c_2\}$

Example 3.5 (Hypersurface regions). Consider the polynomials

$$\begin{aligned} f_1 &= 1 - (x^2 + y^2 + z^2 + w^2) \\ f_2 &= 1 - ((x-1)^2 + y^2 + z^2 + w^2). \end{aligned}$$

Here f_1, f_2 define two Euclidean balls, and $C = \{x \in \mathbb{R}^4 \mid f_1(x) > 0, f_2(x) > 0\}$ their intersection. C is first deformed to C_t for a suitable value of t , and then projected onto the y -axis. The choice of this axis is discussed in Section 4.

Then, at a suitable value of y , the slice is projected onto the x -axis, where the critical points cannot be computed via elimination, due to the occurrence of a positive-dimensional ideal. So, one can employ HypersurfaceRegions.jl to select the correct critical values. Figure 3 shows a 2-dimensional picture of the different regions of the hypersurface arrangement, and the points sampled from each of them.

1DimVolume. If $\dim(C_t) = 2$, then after computing the relevant critical values c_1, c_2 of the projection, the algorithm calls for computing volumes of 1-dimensional slices at $x_i = v$ for $c_1 < v < c_2$. This is done by intersecting the curve F_t with the line $x_i = v$. By convexity, there are only two intersection points that lie inside C . Denote them by λ_1 and λ_2 . Then, the required 1-dimensional volume is $|\lambda_1 - \lambda_2|$.

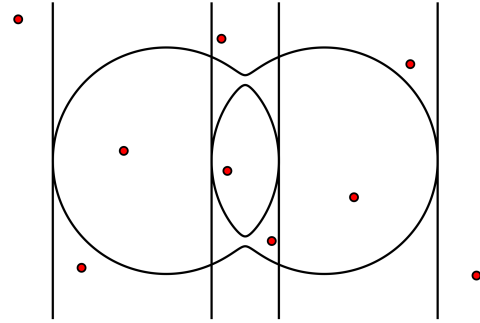


Figure 3: Sampling points to select the correct critical values

SuitableValues. In general, once we have correctly selected the two critical values of a projection, it remains to select the values at which we take slices. Note that a hyperplane $\{x_i = v\}$ for $v \in (c_1, c_2)$ will intersect C_t at more than one point. There may be apparent singularities of the Picard–Fuchs operator P that lie in (c_1, c_2) . Let p_0 be the smallest such singularity. Then, we sample $\text{ord}(P)$ many values (that are not too close) in (c_1, p_0) . These will provide initial conditions to solve P . Although the initial conditions must avoid apparent singularities, the volume function is analytic in the interval (c_1, c_2) and can be continued through any apparent singularities of P .

4 Implementation and experiments

Our implementation of the above algorithms can be found at [15]. It is written mostly in SageMath, building on the `ore_algebra` package to compute Picard–Fuchs operators and to solve them to arbitrary precision. In `CriticalValues` elimination is carried out using `Macaulay2`. Furthermore, `msolve` is used to compute `CritPts` and the intersection points in `1DimVolume`. Finally, when the ideal of the critical locus is positive dimensional, so that it cannot be computed with `msolve`, we use the Julia package `HypersurfaceRegions.jl` [16] to sample points in the complement of $V(F_{t_{\text{val}}}) \cup_{s \in \text{CritVals}} \{x_i = s\}$.

The most expensive step of the volume computation is the process of creative telescoping. Therefore, it is of great interest to minimize the number of times a Picard–Fuchs operator is computed. Let us consider a volume computation for a semi-algebraic set in \mathbb{R}^n . Let d denote the maximum order of all Picard–Fuchs operators computed in the recursive algorithm. The general algorithm in [12] would require a creative telescoping computation for every slice value (at most d) for every pair of adjacent critical values of a projection onto a coordinate axis (recall (16)). If c denotes the maximum number of pairs of adjacent critical values of any projection of a slice, then this would mean the number of creative telescoping steps that are required are bounded above by $(c \cdot d)^n$.

In contrast, by restricting to the class of convex semi-algebraic sets defined by concave polynomials, the number of relevant critical values for any projection is exactly 2, thus requiring only one telescoping step for each slice. Thus, the number of creative telescoping steps is bounded above by d^n . This reduces the general recursive

algorithm, which traverses every node of a tree, to a recursive algorithm on a path. This improves the complexity from the general case by an exponential factor in the dimension n .

Let us now compute exact volumes of various convex bodies. In doing so, we encounter many interesting questions, and opportunities for future work. All of these examples can be reproduced using our implementation by running the Jupyter notebook found at [15].

Example 4.1 (Two Euclidean balls in dimension 4). We continue Example 3.5 and compute the volume of the intersection of two Euclidean balls in 4 dimensions, centered at

$$\mu_1 = (0, 0, 0, 0), \quad \mu_2 = (1, 0, 0, 0).$$

The operator P_t which annihilates $\text{vol}(C_t)$ for small t has order 3 and degree 4. The value of the slices $\text{vol}(C_t)$ are computed for $t \in (0, 5625/10000)$, where $5625/10000$ is the smallest real point in the singular locus of P_t . Projecting in the reverse order of variables, that is x_3, x_2, x_1, x_0 , all subsequent ideals of critical points are zero-dimensional. Finally, the volume is computed to be

$$\begin{aligned} & 1.24934384893295779102649229344462517961832527330926 \\ & 37279549959064283763620392536285226171895009497206 \\ & 44758421633474540092111890318221306407347172357265 \\ & 78794809305528585515475494602146469693898082410815 \\ & 98529998412506559308568339206044582076143683749948 \\ & 5954393910960456071341017606352607002\dots \end{aligned}$$

These are the first 288 decimal digits of the period. The precision of the volume can be decided by the user. We can compare this output with a volume computation using the Monte Carlo method. With 10^8 sample points, we get the volume 1.24952304, which already differs from the exact volume at the 4th decimal place.

We can compute volumes of intersections of a range of convex bodies in reasonable time. Example 4.2 shows truncated exact volumes of some convex bodies in dimensions 2 and 3, and the (average) computation times.

Example 4.2 (More volumes). We compute the volumes of the following convex bodies upto a precision of 10^{-50} :

- (1) A triangle given by $1 - x - y, y, x - y + 1$
- (2) A tetrahedron given by $x, y, z, 1/3 - x - y - z$
- (3) An ellipse and a circle given by $1 - 4x^2 - (y - 1/2)^2, 1 - (x - 1/2)^2 - y^2$
- (4) Two ℓ_4 -balls in \mathbb{R}^2 given by $1 - x^4 - y^4, 1 - (x - 1/2)^4 + y^4$

convex body	volume	time
Triangle	1.0000000000000...	1.1s
Tetrahedron	0.006172839506172839506...	9.2s
Ellipse and circle	1.063610448155437831407...	1m 25.0s
Two ℓ_4 -balls in \mathbb{R}^2	2.708344826299720090001...	3m 56s

There are, however, many examples within our class that do not terminate after days, since the creative telescoping computation becomes too large. Therefore, understanding how the order and degree of the Picard–Fuchs operators change as the input polynomials vary is of interest. We make the following observation:

Example 4.3 (Picard–Fuchs operator of an ℓ_p -ball). We computed Picard–Fuchs operator of a single ℓ_p -ball which annihilates the

volumes of the x_i -slices. We performed this computation for the following values of n and p :

$$\begin{aligned} n = 2, 3 & \quad p \leq 36 \\ n = 4 & \quad p \leq 28. \end{aligned}$$

With the exception of $n = 4, p = 2$, the Picard–Fuchs operator P_{x_i} has the form

$$P_{x_i} = (1 - x_i^p) \partial_{x_i} + (n - 1) x_i^{p-1}. \quad (28)$$

We expect that a general statement can be made here. The case of $n = 4, p = 2$ is discussed in Example 4.6.

In the next two examples, we consider the intersection of two convex bodies in \mathbb{R}^2 . Keeping the first one fixed and moving the second, we take note of changes in the order and the degree of the computed Picard–Fuchs operators.

Example 4.4 (Translating two ℓ_4 -balls). We consider two ℓ_4 -balls in \mathbb{R}^2 centered at $\mu_1 = (0, 0)$ and $\mu_2 = (a, 0)$ for varying a and compute the Picard–Fuchs operator in the deformation parameter t .

For generic values (such as $27/45, 21/20, -1/7, 1$) of a , the operator P_t has order 6 and degree 18. However, for special values of a , the order and degree drop. For $a = 2$ and $a = -2$ we obtain $\text{ord}(P_t) = 6$ and $\text{deg}(P_t) = 17$. We ignore the case of $a = 0$ since that corresponds to a single ℓ_p -ball.

Example 4.5 (Rotating two Euclidean balls). Consider in \mathbb{R}^2 two ℓ_2 -balls with centers $\mu_1 = (0, 0)$ and $\mu_2 = (a, b)$, where μ_2 is a rational point on the unit circle. The Picard–Fuchs operator P_t stays invariant under the choice of μ_2 . This is because the volume is invariant under rotation. However, we see from the following table that the Picard–Fuchs operator P_{x_1} annihilating the x_1 -slices of the deformation C_t for $t = 1/50$ has the same degree and order if $a, b \neq 0$. If either a or b is equal to 0 then both the degree and order drop.

a, b	$\text{ord}(P_{x_1})$	$\text{deg}(P_{x_1})$
1, 0	4	10
0, 1	3	9
-3/5, 4/5	5	17
15/17, 8/17	5	17
8/10, -6/10	5	17

Since the volume of a convex body in \mathbb{R}^n is invariant under the action of $\text{SL}_n(\mathbb{Q})$ and translations, reducing the number of terms of the input polynomials by such a transformation appears to be a strategy to obtain a Picard–Fuchs operator of a lower order. A more concrete understanding of the relationship between the input polynomials and the Picard–Fuchs operators computed could lead to heuristics that aid in computing objects that are currently out of reach, such as the intersection of two ℓ_4 -balls in \mathbb{R}^4 . It is worth studying if it is possible to bypass heavy creative telescoping computations by utilizing the explicit structure of the ℓ_p -polynomials.

We conclude with a comment on the choice of the creative telescoping algorithm. In our current implementation, creative telescoping is carried out via the implementation of Chyzak’s algorithm [5] in the `ore_algebra` package. While in Theorem 2.4, the integration ideal is computed over the Weyl algebra $D_{t,x}$, Chyzak’s algorithm actually computes elements in

$$(J + \partial_{x_1} R_{t,x} + \dots + \partial_{x_n} R_{t,x}) \cap R_t, \quad (29)$$

so that differential operators with rational coefficients are also allowed. This leads in some cases to unwanted behaviors. If the certificates of the creative telescoping process have *spurious* poles, i.e. poles other than f and powers of f , then the proof of Theorem 2.4 does not hold. As a consequence, the computed Picard–Fuchs operator may not actually annihilate the period integral as the following extreme example, found in [13], shows:

Example 4.6 (Spurious poles). Consider a single Euclidean ball in \mathbb{R}^4 defined by $C = \{x \in \mathbb{R}^4 \mid f(x) > 0\}$ for $f = 1 - (x_1^2 + x_2^2 + x_3^2 + x_4^2)$. Then,

$$A = \frac{(\partial_1 \bullet f)x_1}{f} = -\frac{2x_1^2}{f}$$

denotes the rational function whose periods describe the volume of, for example, the x_4 -slices of C . However, the R_{x_4} ideal

$$I = (\text{Ann}_{R_x}(A) + \partial_{x_1}R_x + \partial_{x_2}R_x + \partial_{x_3}R_x) \cap R_{x_4} \quad (30)$$

contains the operator 1, since the rational function A can be decomposed as a sum of derivatives

$$3A = \partial_1 \bullet \frac{2x_1^3}{f} + \partial_2 \bullet \frac{2x_1^4 x_2}{f \cdot (x_4^2 + x_1^2 - 1)} + \partial_3 \bullet \frac{2x_3 x_1^4}{f \cdot (x_4^2 + x_1^2 - 1)}.$$

From the above equation, we see that for the telescoper $P = 1$ and certificates

$$Q_1 = \frac{x_1}{3}, \quad Q_2 = \frac{x_1^2 x_2}{3(x_4^2 + x_1^2 - 1)}, \quad Q_3 = \frac{x_1^2 x_3}{3(x_4^2 + x_1^2 - 1)}$$

the differential operator

$$P - \partial_1 Q_1 - \partial_2 Q_2 - \partial_3 Q_3$$

annihilates A . However, P clearly does not annihilate the periods of A , since the slices of C have non-zero volume. This is not a contradiction to Theorem 2.4 since here the certificates do not lie in D_x .

A more subtle example of unexpected behavior is the following:

Example 4.7 (Singular locus of Picard–Fuchs operator). Consider two ℓ_2 -balls centered at $\mu_1 = (0, 0, 0, 0)$ and $\mu_2 = (1, 0, 0, 0)$ as in Example 3.5, the projection of the deformation for $t = 1/1000$ onto the x_0 axis gives the Picard–Fuchs operator 1.

If we change the order of projection and project the deformation first onto the x_1 axis, we get Picard–Fuchs operator of degree 10 and order 3. For $x_1 = -7/10$, we project onto the x_0 axis. Here we encounter a different problem. The singular locus of the operator should contain the critical values of the projection due to the fact that at the critical values, the number of connected components of the fiber changes. This shows us that the computed operator does not annihilate the period.

To avoid issues such as those in the above examples, the implementation allows the input of a custom order of projections via the routine `ProjectionVariable`. For two ℓ_2 balls in \mathbb{R}^4 , the projection order in Example 4.1 avoids these issues. To avoid these issues altogether, one could instead call a creative telescoping algorithm that works in D_x , such as implemented in the software package `MultivariateCreativeTelescoping.jl` [4]. Another avenue to avoid these unwanted behaviors is to use an algorithm that avoids poles

outside $V(F_t)$. We expect that advances in creative telescoping algorithms will allow to compute volumes of objects that are currently out of reach.

References

- [1] Jérémie Berthomieu, Christian Eder, and Mohab Safey El Din. 2021. *msolve: A Library for Solving Polynomial Systems*. In *2021 International Symposium on Symbolic and Algebraic Computation* ACM, 51–58.
- [2] Jeff Bezanson, Alan Edelman, Stefan Karpinski, and Viral B Shah. 2017. Julia: A fresh approach to numerical computing. *SIAM review* 59, 1 (2017), 65–98.
- [3] Paul Breiding, Kathlén Kohn, and Bernd Sturmfels. 2024. *Metric Algebraic Geometry*. Birkhäuser.
- [4] Hadrien Brochet, Frédéric Chyzak, and Pierre Lairez. 2025. Faster multivariate integration in D -modules. Preprint [arXiv:2504.12724](https://arxiv.org/abs/2504.12724)
- [5] Frédéric Chyzak. 2000. An extension of Zeilberger’s fast algorithm to general holonomic functions. *Discrete Math.* 217, 1–3 (2000), 115–134.
- [6] Frédéric Chyzak. 2014. *The ABC of Creative Telescoping – Algorithms, Bounds, Complexity*. Ecole Polytechnique X. Accreditation to supervise research.
- [7] Daniel R. Grayson and Michael E. Stillman. *Macaulay2*, a software system for research in algebraic geometry. Available at <http://www2.macaulay2.com>
- [8] Manuel Kauers. 2023. *D-finite functions*. Algorithms and Computation in Mathematics, Vol. 30. Springer.
- [9] Manuel Kauers, Maximilian Jaroschek, and Fredrik Johansson. 2015. Ore polynomials in Sage. In *Computer algebra and polynomials*. Lecture Notes in Comput. Sci., Vol. 8942. Springer, 105–125.
- [10] Vladimir Koltchinskii, Lakshmi Ramesh, and Martin Wahl. 2026. Maximum likelihood estimation of the location of a symmetric convex body. Manuscript in preparation.
- [11] Pierre Lairez. 2016. Computing periods of rational integrals. *Math. Comp.* 85, 300 1719–1752.
- [12] Pierre Lairez, Marc Mezzarobba, and Mohab Safey El Din. 2019. Computing the Volume of Compact Semi-Algebraic Sets. *Proceedings of the 2019 International Symposium on Symbolic and Algebraic Computation (ISSAC ’19)*. ACM, 259–266.
- [13] Marc Mezzarobba. 2023. *volumes*. A Git repository available at <https://src.koda.cnrs.fr/marc.mezzarobba.3/volumes/>.
- [14] Frédéric Pham. 2011. *Singularities of integrals*. Springer, EDP Sciences.
- [15] Lakshmi Ramesh and Nicolas Weiss. 2026. *exact_convex_volumes: v0.0.1*. <https://doi.org/10.5281/zenodo.18472470>
- [16] Bernhard Reinke and Kexin Wang. 2024. Hypersurface Arrangements with Generic Hypersurfaces Added. Preprint [arXiv:2412.20869](https://arxiv.org/abs/2412.20869)
- [17] Mutsumi Saito, Bernd Sturmfels, and Nobuki Takayama. 2000. *Gröbner deformations of hypergeometric differential equations*. Algorithms and Computation in Mathematics, Vol. 6. Springer.
- [18] Anna-Laura Sattelberger and Bernd Sturmfels. 2025. *D*-Modules and Holonomic Functions. In *Varieties, Polyhedra, Computation*. EMS Series of Congress Reports, Vol. 22. EMS Press, 251–293.
- [19] Nobuki Takayama. 2013. Gröbner Basis for Rings of Differential Operators and Applications. In *Gröbner Bases: Statistics and Software Systems*, Takayuki Hibi (Ed.). Springer, 279–344.
- [20] The Sage Developers. 2025. *SageMath, the Sage Mathematics Software System (Version 10.6)*. <https://www.sagemath.org>
- [21] D. Zeilberger. 1990. A holonomic systems approach to special functions identities. *Journal of Computational and Applied Mathematics*, 32(3):321–368.